ISSN 1330–0016
CODEN FIZBE7

STUDY OF ^{194}Ir VIA THERMAL NEUTRON CAPTURE AND (d,p) REACTIONS

M. BALODIS, P. PROKOFJEVS, N. KRAMERE, L. SIMONOVA, J. BERZINS, T. KRASTA,
Nuclear Research Center, LV-2169 Salaspils, Latvia

R. GEORGII, T. von EGIDY, J. KLORA, H. LINDNER, U. MAYERHOFER, A. WALTER,
Physik-Department, E18, Technische Universität München, D-85748 Garching bei München, Germany

J. A. CIZEWSKI,
Rutgers University, Piscataway, NJ 08855, USA

G. G. COLVIN, H. G. BOERNER, P. GELTENBORT, F. HOYLER, S. A. KERR, K. SCHRECKENBACH,
Institute Laue-Langevin, F-38042 Grenoble, France

A. RAEMY, J. C. DOUSSE, J. KERN, W. SCHWITZ,
Physics Department, University of Fribourg, CH-1700 Fribourg, Switzerland

I. A. KONDUROV, YU. E. LOGINOV, P. A. SUSHKOV,
Petersburg Nuclear Physics Institute, 188350 Gatchina, Russia

S. BRANT, V. PAAR
Department of Physics, University of Zagreb, HR-10000 Zagreb, Croatia

and V. LOPAC
Department of Physics, Faculty of Chemical Engineering and Technology, University of Zagreb, HR-10000 Zagreb, Croatia

Received 28 August 1997; Accepted 11 May 1998

Levels of ^{194}Ir were studied using thermal neutron capture reaction. A pair spectrometer was used to measure the high-energy γ-ray spectrum from thermal-neutron capture in enriched ^{193}Ir target over the energy range 4640 – 6100 keV. The low-energy γ-radiation

from the reaction was studied with crystal diffraction spectrometers, and conversion electrons were observed with magnetic spectrometers. The high-sensitivity measurements at the Grenoble reactor, evaluated for transition energies up to 500 keV, are compared with lower-sensitivity measurements at the Wuerenlingen and Salaspils reactors. The comparison helped to obtain reliable isotopic identification for a number of ^{194}Ir lines. The multipolarity admixtures for 29 γ-transitions were determined on the basis of conversion lines from different electron subshells. Prompt and delayed γ-γ coincidences were measured using semiconductor and scintillation detectors. The ^{193}Ir(d,p) high-resolution spectra, observed with a magnetic spectrometer, are given. All these data contributed to establishing a detailed level scheme of ^{194}Ir. Additional data and the interpretation of the results in terms of current models will be presented in a forthcoming paper.

PACS numbers: 21.10-k, 23.20Lv, 27.80+w UDC 539.163, 539.172

Keywords: ^{194}Ir levels, (n,γ) and (d,p) reactions, γ-ray spectra, diffraction spectrometer, magnetic spectrometers, prompt and delayed γ-γ coincidences

1. Introduction

Nuclei in the Os–Ir–Pt region have been intensively studied using both experimental and theoretical methods for quite a long time. Interpretation of the structure of these nuclei requires a complicated model approach. It is generally accepted that nuclei in this region are successfully described using the O(6) limit of IBA. For odd-odd nuclei, it means the application of the boson-fermion-fermion model in the O(6) limit. Nevertheless, some features, compatible with small surface deformation, allow also a level-structure interpretation within the framework of the Bohr-Mottelson-Nilsson model, though the limitations of that approach are hard to define precisely. The detailed study of low-energy level schemes for the nuclei of this region would help very much to clarify this point.

The ^{194}Ir nucleus, situated in a transitional region between the strongly deformed $A = 155$–185 nuclei and the doubly magic ^{208}Pb nucleus, should provide useful tests of current models. Though both ^{192}Ir and ^{194}Ir can be excited by neutron capture with relatively large thermal capture cross-sections (954(10) and $111(5)\cdot 10^{-28}$ m^2, respectively), a level scheme with a detailed model interpretation of ^{192}Ir has not been developed until recently [1]. Previous publications on ^{194}Ir include neutron-capture results [2], presented without a level-scheme interpretation, observation of the ^{194}Os beta-decay [3–5] and measurements of decay of a 32 ms isomeric state [6,7].

For ^{194}Ir, the observation of neutron-capture spectra is the best experimental method since it allows to find almost all low-energy levels up to a few hundreds of keV. A larger cooperation was undertaken some time ago to study ^{194}Ir, using a wide scope of experimental data. Besides the (n,γ) and (n,e$^-$) measurements, results of our study include also data on average resonance (ARC) neutron-capture spectra and the results of the (d,p) reaction measurements. The main results of this collaboration are published in Ref. 8. Preliminary results were reported at several conferences (e.g. Refs. 9–11). The recent (d,p)

work of Garrett et al. [12] took into account these preliminary results. Though Garrett et al. have disclosed several important features of ^{194}Ir, a detailed insight into the structure of this nucleus is still missing.

In Ref. 8 are given the main experimental results leading to a level scheme and to a structure interpretation. However, for a nucleus of such complexity, we feel important to publish complete results, obtained in the process of our studies, although they are not crucial for the understanding of the ^{194}Ir level scheme. These data include: (i) the full energy range of primary γ-rays, which in Ref. 8 is given only up to 600 keV excitation energy; (ii) the low-energy γ-rays and conversion electrons detected with a lower neutron flux, compared to the same transitions observed with a higher flux of measurements described in Ref. 8; (iii) the multipolarity mixings supported by subshell electron intensities; (iv) the detailed account of results of γ-γ coincidences; (v) the full energy range of (d,p) reaction spectra, obtained using 22 MeV deuterons, which in Ref. 8 is cut at 600 keV excitation energy.

2. Experimental methods and results

2.1. Primary γ-rays from thermal neutron capture (Fribourg-Wuerenlingen)

The ^{193}Ir(n,γ)^{194}Ir primary γ-rays were observed with a pair spectrometer [13], placed at the SAPHIR reactor of EIR (now Paul Scherrer Institute) at Wuerenlingen. The external target, enriched to 98.1% in ^{193}Ir, of a mass of 20 mg, was placed in the thermal neutron flux of 2×10^7 n cm^{-2} s^{-1}. In order to identify the lines from capture in ^{191}Ir, measurements with a 37 mg target enriched to 86% in ^{191}Ir and with a 4 g sample of natural iridium were performed (see also Ref. 1). The ^{194}Ir results, extending up to 1430 keV excitation energy, are listed in Table 1. Level energies were determined from the primary γ-ray energies with the help of the neutron separation energy $B_n = 6066.9(2)$ keV (see Ref. 8).

2.2. Low-energy (n,γ) measurements (Fribourg-Wuerenlingen)

Measurements with a Compton suppression spectrometer and with a single Ge(Li) detector were performed using 15 mg and 150 mg natural Ir targets. The comparison of these measurements with the results obtained with the 37 mg sample enriched to 86% in ^{191}Ir provided identification and intensity calibration of a few intensive ^{194}Ir transitions.

The ^{193}Ir(n,γ)^{194}Ir spectrum was also observed from 43 to 520 keV with a curved crystal spectrometer [14–17] at Wuerenlingen. The 30 mg target had a 98.7% ^{193}Ir

TABLE 1. Primary transitions from the ^{193}Ir(n,γ) *reaction, observed with a pair spectrometer, and the levels of* ^{194}Ir*, computed assuming* $B_n = 6066.9 \pm 0.2$ keV.

E_γ (keV)	I_γ (rel)	E_{exc} (keV)	E_γ (keV)	I_γ (rel)	E_{exc} (keV)
6067.00±0.40	12.2±1.1	0.0 ±0.35	5281.77±0.68	6.4±1.1	785.1 ±0.60
6023.85±1.50	3.3±1.4	43.1 ±1.50	5264.82±0.98	6.5±4.0	802.1 ±0.90
5984.17±0.47	11.4±2.0	82.7 ±0.40	5261.06±0.88	7.0±2.0	805.8 ±0.80
5954.67±0.42	27.9±3.5	112.2 ±0.35	5246.60±0.97	4.9±2.8	820.3 ±0.90
5928.15±0.36	10.0±2.2	138.7 ±0.30	5231.60±0.60	3.6±1.5	835.3 ±0.50
5918.15±0.37	12.2±1.6	148.7 ±0.30	5189.45±0.97	5.5±2.2	877.45±0.90
5904.97±0.66	7.2±1.6	161.9 ±0.60	5180.70±0.63	12.2±3.0	886.2 ±0.60
5882.50±0.63	6.8±1.6	184.4 ±0.60	5158.40±0.62	7.0±2.7	908.5 ±0.60
5821.45±0.40	22.2±2.0	245.45±0.35	5140.10±0.85	5.2±1.0	926.8 ±0.80
5814.00±0.80	5.0±1.7	252.9 ±0.70	5128.95±0.77	6.6±1.1	938.0 ±0.70
5787.38±0.48	18.7±3.5	279.5 ±0.40	5109.74±0.64	7.2±3.0	957.2 ±0.60
5757.45±1.70	2.2±1.5	309.45±1.70	5090.63±0.68	9.1±1.1	976.3 ±0.60
5750.08±1.70	2.1±1.5	316.8 ±1.70	5071.85±0.50	14.4±2.0	995.0 ±0.40
5728.73±0.32	38.0±3.5	338.2 ±0.25	5028.16±0.48	17.8±4.0	1038.7 ±0.40
5678.03±1.40	2.2±1.5	388.9 ±1.40	5014.40±0.90	12.2±3.5	1052.5 ±0.80
5643.53±0.37	13.6±1.5	423.4 ±0.30	4991.83±1.10	4.9±1.4	1075.1 ±1.10
5630.70±0.36	15.0±1.6	436.2 ±0.30	4979.50±0.76	7.9±1.6	1087.4 ±0.70
5577.14±0.44	6.6±1.9	489.75±0.40	4967.65±0.72	6.8±2.8	1099.25±0.70
5563.47±0.63	10.7±1.5	503.4 ±0.60	4930.81±0.86	8.8±2.4	1136.1 ±0.80
5519.20±1.20	9.3±3.0	547.7 ±1.20	4892.35±1.00	4.5±2.7	1174.55±1.00
5487.62±0.54	14.2±1.3	579.3 ±0.50	4875.41±1.20	4.7±2.0	1191.5 ±1.20
5466.65±0.48	23.2±6.0	600.25±0.40	4855.47±0.59	13.3±2.3	1211.4 ±0.50
5385.88±0.90	4.8±1.8	681.0 ±0.80	4839.30±0.52	12.3±2.2	1227.6 ±0.40
5368.00±0.80	2.7±1.3	698.9 ±0.70	4827.20±0.72	8.8±2.1	1239.7 ±0.70
5357.92±0.50	18.0±3.0	709.0 ±0.40	4808.32±0.70	6.9±1.4	1258.6 ±0.60
5315.35±0.65	11.0±2.4	751.55±0.60	4754.75±0.44	16.1±3.0	1312.15±0.40
5300.32±1.10	6.6±2.0	766.6 ±1.10	4643.40±0.60	12.1±2.1	1423.5 ±0.50
5291.20±0.53	6.4±1.7	775.7 ±0.40			

enrichment. Table 2 shows 101 γ-ray transitions assigned to ^{194}Ir. More detailed information on the Fribourg-Wuerenlingen ^{192}Ir and ^{194}Ir measurements for high and low γ-ray energies can be found in Ref. 1 and in Ref. 18.

In Table 2, a comparison is given with the partial results of low-energy γ-ray measurements in ILL (Grenoble) (for complete data see Ref. 8), which are of a higher sensitivity than the Fribourg-Wuerenlingen data. Nevertheless, the analysis of the results justifies the publication of all data listed in Table 2: (i) the intensity calibration vs. energy is more precise for the Wuerenlingen results, at least for the strongest lines; (ii) since the neutron flux in Grenoble (5.5×10^{14} n cm^{-2} s^{-1}) is more than an order of magnitude higher than that at the Wuerenlingen reactor (3×10^{13} n cm^{-2} s^{-1}), it was necessary to make a complicated isotopic identification of the ^{194}Ir and ^{195}Ir lines for the ILL results. Such identification is not 100% reliable. An observation of the line in Wuerenlingen is a strong argument for its assignment to ^{194}Ir. This provides also a means for testing the identification procedure used with the ILL data. The same arguments, at least partly, are also valid for the conversion electron data (Tables 2 and 3).

All intensity scales in Table 2 are reduced to relative intensities used in Ref. 18 as

well as in Ref. 19. This scale is based on setting $I_\gamma = 100$ for the intensive 112.2 keV transition. In order to obtain the scale of column 2, the earlier relative intensity scale of the Grenoble data, used in a laboratory report [20] (see also Ref. 21), has been divided by 9 to give comparable intensities for the 82, 84, 112, 123, 138, 148 and 184 keV transitions.

TABLE 2. Secondary γ-rays and transition multipolarities observed and deduced on a basis of four series of measurements. In columns 1,2 and 6, selected sets of Grenoble measurements [8] are given. The measurements at Wuerenlingen (Sect. 2.2) and the conversion electron measurements at Riga (Sect. 2.3) are presented in columns 3,4,5 and 7. Standard errors in terms of last digits are given in parentheses.

Gamma-rays (Grenoble)		Gamma-rays (Wuerenlingen)		Internal conversion (Riga-Salaspils)[a]	Internal conversion (Grenoble)[b]	Multi-pola-rity[c]
E_γ (keV)	I_γ (rel.)	E_γ (keV)	I_γ (rel.)			
[d]29.890 (6)	[d]1.9 (1.8)			L_1, M_1, N_1	L_1=13.1(18)	[f]M1
[e]34.829 (10)	- -			L_1, L_3, M_1, M_3	$L_{1-3}, M_{1-3}, N_{1-3}$	[f]M2
39.217 (1)	8.3 (5)			L_1, L_2, M_1, N_1	L_1=12.9(12)	[f]M1
43.119 (1)	37.3 (26)	43.117 (3)	48 (12)	$L_1 = 13(4), L_2, L_3, M_1, M_2, N_1, O_1$	L_1=9.56(83)	M1
54.401 (1)	[d]5.9 (5)			L_1, M_1	L_1 =5.26(61)	(M1)
62.793 (3)	1.6 (2)			$L_1 = 98(17), L_2, L_3, M_1, M_3, N_1, N_3$	L_1=68.7(103)	M2
82.339 (2)	24.0 (4)	82.335 (4)	17 (4)	$L_1 = 1.7(5), M_1$	$L_1 = 1.35(9)$	M1
84.288 (2)	55.5 (36)	84.280 (2)	52 (6)	$L_1 = 1.06(15), L_2, L_3, M_1, M_2, M_3$	$L_1 = 1.06(9)$	M1+ E2
93.166 (2)	16.6 (4)	93.156 (4)	18 (4)	$K = 5.7(14), L_1, M_1$	$L_1 = 0.96(8)$	M1
95.575 (3)	38.5 (17)	95.563 (3)	33 (5)	$K = 5.5(14), L_1, M_1$	$K = 5.17(26)$	M1
112.230 (1)	96.7 (17)	112.2290 (12)	100 (8)	$K = 1.89(27), L_1, L_2, L_3, M_1, M_2, M_3, N, O$	$K = 1.30(7)$	M1+ E2
113.447 (1)	4.5 (1)	113.420 (15)	5.2 (16)	$K = 2.7(11), L_1$	$K = 3.50(22)$	M1
115.473 (1)	22.5 (5)	115.464 (4)	25 (4)	$K = 1.9(5), L_1$	$K = 3.65(21)$	M1
117.880 (2)	20.6 (8)	117.874 (4)	22 (4)	$K = 2.0(6), L_1$	$K = 3.5(2)$	M1
123.845 (1)	48.3 (15)	123.839 (3)	47 (5)	$K = 2.5(6), L_1$	$K = 2.76(16)$	M1
132.883 (2)	8.4 (3)	132.872 (6)	11.6 (23)	$K = 1.3(4), L_1$	$K = 0.84(6)$	M1

Table 2. (continued)

Gamma-rays (Grenoble)		Gamma-rays (Wuerenlingen)		Internal conversion (Riga-Salaspils)[a]	Internal conversion (Grenoble)[b]	Multi-polarity[c]
E_γ (keV)	I_γ (rel.)	E_γ (keV)	I_γ (rel.)			
136.100 (2)	8.1 (5)	136.116 (4)	15.7 (23)	$K = 1.4(7)$		M1
138.686 (1)	38.7 (7)	138.689 (3)	45 (4)	$K = 0.89(20), L_1, L_2, L_3, M_{12}, M_3$	$K = 1.07(8)$	M1+ E2
142.119 (2)	5.1 (4)	142.144 (18)	7 (4)	$K = 1.7(6)$	$K = 1.76(23)$	M1
142.199 (6)	3.1 (2)				$K = 1.90(21)$	
143.594 (1)	30.8 (4)	143.590 (3)	35 (4)	$K = 1.4(2), L_1$	$K = 1.86(9)$	M1
145.221 (2)	5.2 (2)	145.214 (12)	6.9 (17)	$K = 0.55(31)$	$K = 1.80(19)$	E2, M1
146.169 (2)	4.3 (2)	146.202 (20)	4.5 (14)	$K = 2.3(10)$	$K = 2.5(3)$	M1
147.630 (9)	2.4 (5)					
147.979 (3)	2.2 (1)	147.946 (40)	4.8 (14)			
148.934 (1)	68.4 (17)	148.932 (3)	73 (6)	$K = 0.33(8), L_1, L_2, L_3, M_2, M_3, N_{23}$	$K = 0.42(3)$	E2
152.405 (2)	17.6 (4)	152.400 (6)	17.8 (27)	$K = 0.14(4)$	$K = 0.42(4)$	E1, E2[g]
153.054 (1)	23.7 (6)	153.049 (5)	26 (3)	$K = 1.7(4), L_1, M_1$	$K = 1.55(12)$	M1
160.825 (2)	16.2 (4)	160.818 (6)	13.8 (21)	K, L_1, L_2, L_3[h)]	$K = 0.66(7)$	M1+ E2[h]
160.996 (2)	20.1 (4)	160.992 (4)	22 (3)	K, L_1, L_2, L_3[h)]	$K = 0.68(10)$	M1+ E2[h]
161.507 (10)	1.0 (2)					
162.366 (3)	2.4 (1)	161.961 (10)	4.4 (13)			
162.774 (2)	11.5 (3)	162.770 (10)	9.8 (20)	$K = 0.67(34)$	$K = 0.30(3)$	M1+ E2
165.374 (3)	12.9 (5)	165.359 (13)	9.3 (14)	K, L_1[h)]	$K = 1.20(9)$	M1[h]
165.448 (3)	16.9 (5)	165.431 (7)	17.1 (21)	K, L_1[h)]	$K = 1.27(13)$	M1[h]
166.275 (3)	4.6 (1)	166.260 (30)	5.0 (15)			
		169.539 (13)	9.3 (14)			
169.564 (2)	11.3 (3)			K	$K = 1.18(9)$	M1

Table 2. (continued)

Gamma-rays (Grenoble)		Gamma-rays (Wuerenlingen)		Internal conversion (Riga-Salaspils)[a]	Internal conversion (Grenoble)[b]	Multi-polarity[c]
E_γ (keV)	I_γ (rel.)	E_γ (keV)	I_γ (rel.)			
		169.662 (35)	12.6 (25)			
169.874 (2)	7.4 (3)	169.857 (20)	5.9 (18)	$K = 1.5(5)$	$K = 1.16(10)$	M1
176.654 (3)	7.5 (2)	176.645 (40)	7.0 (18)	$K = 0.53(18)$	$K = 1.13(14)$	M1
179.226 (3)	4.3 (2)	179.150 (45)	7.6 (19)	$K = 0.13(6)$	$K = 0.95(8)$	
180.930 (5)	2.4 (1)	181.000 (80)	4.0 (12)			
181.069 (5)	2.1 (2)					
182.146 (5)	4.3 (1)	182.142 (30)	4.0 (12)			
184.687 (2)	44.0 (8)	184.684 (6)	35.7 (18)	$K = 0.22(5)$, L_1, L_2, L_3	$K = 0.19(1)$	E2
186.162 (3)	4.3 (1)	186.169 (50)	2.9 (15)			
193.928 (3)	10.1 (3)	193.915 (13)	9.0 (18)	$K = 0.70(20)$	$K = 0.67(6)$	E2
195.519 (3)	10.0 (3)	195.507 (18)	9.4 (19)	$K = 0.35(10)$	$K = 0.18(2)$	M1+ E2
198.834 (3)	7.0 (1)	198.753 (80)	5.4 (19)			
204.187 (3)	4.2 (1)	204.164 (50)	5.2 (16)	$K = 0.5(2)$	$K = 0.61(5)$	M1+ E2
211.133 (4)	2.8 (2)	211.173 (30)	4.7 (30)	$K = 1.0(5)$	$K = 0.53(8)$	M1
212.346 (2)	7.4 (2)	212.373 (30)	7.7 (19)			
216.903 (6)	2.0 (2)	216.874 (70)	6.5 (20)			
219.163 (2)	8.8 (4)	219.420 (120)	4.2 (13)	$K = 0.9(4)$	$K = 0.12(2)$	M1
224.085 (3)	8.6 (4)	224.073 (30)	7.4 (19)	K	$K = 0.51(4)$	
225.412 (5)	5.5 (1)	225.390 (50)	7.2 (18)	$K = 1.0(4)$	$K = 0.39(4)$	M1
226.299 (15)	1.8 (2)	226.265 (60)	2.0 (10)			
226.639 (2)	9.3 (3)	226.579 (20)	6.7 (20)	$K = 0.48(18)$	$K = 0.42(3)$	M1+ E2
228.070 (4)	5.7 (4)					
		228.186 (45)	7.3 (18)			

Table 2. (continued)

Gamma-rays (Grenoble)		Gamma-rays (Wuerenlingen)		Internal conversion (Riga-Salaspils)[a]	Internal conversion (Grenoble)[b]	Multi-pola-rity[c]
E_γ (keV)	I_γ (rel.)	E_γ (keV)	I_γ (rel.)			
228.201 (4)	4.7 (2)					
231.901 (3)	5.7 (2)	231.873 (60)	5.6 (17)	$K = 0.50(20)$	$K = 0.43(3)$	M1
234.817 (2)	21.2 (5)	234.803 (14)	18.1 (22)	$K = 0.50(11)$	$K = 0.33(3)$	M1
235.493 (5)	3.8 (2)					
		235.569 (40)	8.7 (22)			
235.707 (4)	4.2 (2)					
241.759 (4)	3.7 (2)	241.665 (90)	2.4 (12)			
242.314 (3)	5.1 (2)	242.332 (60)	5.9 (18)			
245.115 (3)	6.7 (3)	245.119 (25)	9.2 (23)	$K = 0.25(9)$	$K = 0.14(2)$	M1+ E2
245.491 (2)	14.5 (3)	245.514 (14)	15.8 (24)	$K = 0.32(9)$	$K = 0.30(2)$	M1+ E2
245.943 (4)	3.6 (2)					
		246.022 (45)	5.4 (16)			
246.051 (8)	1.9 (2)					
248.599 (2)	11.4 (2)	248.616 (95)	11.2 (22)	$K = 0.20(8)$	$K = 0.35(2)$	M1+ E2
250.686 (6)	2.3 (1)	250.683 (75)	4.3 (13)			
252.288 (4)	5.2 (2)	252.263 (50)	9.8 (25)			
255.313 (4)	17.1 (7)	255.350 (18)	14.7 (22)	$K = 0.190(66)$	$K = 0.19(2)$	M1+ E2
262.739 (3)	6.5 (3)	262.722 (70)	5.9 (18)	$K = 0.8(4)$	$K = 0.18(2)$	M1
264.744 (3)	37.5 (9)	264.749 (13)	32.1 (30)	$K = 0.22(8)$	$K = 0.22(1)$	M1+ E2
267.835 (2)	9.4 (3)	267.797 (45)	9.8 (20)			
271.676 (3)	26.8 (5)	271.661 (20)	23.2 (23)	$K = 0.188(66)$	$K = 0.077(55)$	M1+ E2
275.292 (2)	27.0 (4)	275.282 (17)	24.2 (24)	$K = 0.30(8)$	$K = 0.27(1)$	M1
278.502 (3)	84.7 (21)	278.518 (8)	91 (7)	K=0.184(38)	$K = 0.26(2)$	M1+ E2

Table 2. (continued)

Gamma-rays (Grenoble)		Gamma-rays (Wuerenlingen)		Internal conversion (Riga-Salaspils)[a]	Internal conversion (Grenoble)[b]	Multi-polarity[c]
E_γ (keV)	I_γ (rel.)	E_γ (keV)	I_γ (rel.)			
288.423 (8)	5.5 (3)	288.406 (50)	5.9 (18)			
294.411 (28)	3.6 (15)				$K = 0.28(11)$	
		294.474 (18)	20.5 (21)	$K = 0.22(8)$		M1+ E2
294.531 (6)	19.4 (8)				$K = 0.11(1)$	
304.666 (4)	6.5 (2)	304.711 (80)	6.0 (18)	K	$K = 0.20(2)$	
308.975 (2)	27.2 (7)	308.944 (20)	27.4 (27)	$K = 0.124(34)$	$K = 0.16(1)$	M1+ E2
310.594 (2)	12.9 (3)	310.544 (70)	7.0 (21)			
311.492 (4)	7.7 (2)	311.557 (80)	6.3 (19)	K	$K = 0.16(1)$	
314.065 (6)	12.6 (9)	314.141 (30)	18.0 (22)			
324.265 (3)	8.7 (3)	324.250 (90)	7.5 (22)			
324.988 (3)	14.1 (5)	325.028 (45)	12.9 (26)	K	$K = 0.18(1)$	
330.418 (3)	8.1 (3)	330.443 (70)	11.8 (24)	$K = 0.38(18)$	$K = 0.20(2)$	M1
335.095 (6)	4.8 (2)	335.200 (60)	4.3 (13)			
337.531 (4)	29.3 (6)	337.531 (35)	26.8 (32)	$K = 0.078(42)$	$K = 0.15(1)$	M1+ E2
340.813 (4)	36.4 (6)	340.793 (20)	38.7 (47)	$K = 0.186(46)$	$K = 0.16(1)$	M1
342.162 (8)	3.0 (2)	342.205 (70)	6.4 (19)			
347.064 (5)	4.3 (2)	347.025 (70)	9.7 (24)			
353.963 (2)	24.5 (7)	353.948 (25)	27.6 (48)	$K = 0.09(4)$	$K = 0.16(1)$	M1+ E2
360.423 (3)	13.5 (3)	360.451 (70)	13.4 (34)			
371.502 (2)	100.7 (26)	371.443 (16)	105.3 (12)	K=0.036(12)	$K = 0.033(3)$	E2
383.676 (3)	17.0 (5)	383.630 (75)	18.1 (36)	$K = 0.11(6)$	$K = 0.11(1)$	M1
390.961 (2)	27.5 (6)	390.953 (90)	26 (7)	$K = 0.10(4)$	$K = 0.10(1)$	M1
414.783 (3)	29.3 (7)	414.778 (70)	37 (6)	$K = 0.11(4)$	$K = 0.095(4)$	M1

Table 2. (continued)

Gamma-rays (Grenoble)		Gamma-rays (Wuerenlingen)		Internal conversion (Riga-Salaspils)[a]	Internal conversion (Grenoble)[b]	Multi-polarity[c]
E_γ (keV)	I_γ (rel.)	E_γ (keV)	I_γ (rel.)			
418.144 (3)	29.0 (8)	418.078 (60)	37 (6)	$K = 0.04(2)$	$K = 0.105(5)$	M1+ E2
424.323 (46)	1.2 (2)	424.31 (14)	9.4 (28)			
425.444 (12)	2.4 (3)	425.95 (14)	9.2 (30)			
435.840 (9)	4.3 (3)	435.979 (90)	4.1 (20)			
440.458 (10)	10.5 (4)	440.609 (75)	16 (4)			
458.294 (5)	19.6 (4)	458.73 (20)	32 (6)			
460.250 (4)	37.3 (9)	460.104 (70)	51 (6)	$K = 0.024(12)$	$K = 0.010(1)$	E1, E2
467.413 (6)	11.5 (4)	467.815 (90)	39 (6)			
471.581 (8)	9.7 (6)					
472.102 (10)	10.1 (5)	471.86 (20)	17 (5)			
487.176 (6)	26.6 (6)	487.109 (90)	41 (8)	$K = 0.072(36)$	$K = 0.063(3)$	M1
492.744 (79)	4.2 (9)	494.85 (20)	14 (7)			
496.818 (40)	2.1 (3)	496.35 (15)	21 (7)			

Comments to Table 2:

[a]The largest observed ICC value and a list of other electron lines observed for this transition are given; in some cases only observed shells are listed. For transition energies above 184.6 keV the ICC values are reevaluated with respect to earlier data [19].

[b]The largest observed conversion coefficient is given; for 34.8 keV transition – observed shells.

[c]The multipolarity given here is deduced from the ICC values obtained in Riga measurements, unless they contradict the data obtained at Grenoble (compare Table 3).

[d]The γ-ray energies and intensities measured in Gatchina.

[e]The γ-ray energies deduced from Grenoble conversion electron data [8].

[f]The multipolarities based on subshells.

[g]E1 follows from Riga data, E2 from Grenoble results.

[h]For conversion electron lines observed as doublets, the multipolarities are evaluated approximately.

2.3. Conversion electron measurements (Riga & Grenoble)

The internal conversion electron spectrum from thermal-neutron capture in ^{193}Ir was studied with the magnetic beta-spectrograph [22], installed at the tangential channel of the IRT reactor at the Physics Institute (now the Nuclear Research Center), Latvian Academy of Sciences, in Salaspils near Riga. The targets, located near the reactor core, were exposed to a neutron flux of 3.2×10^{12} n cm^{-2} s^{-1}. The targets consisted of enriched metallic iridium evaporated on aluminium foils 0.74 μm thick. The ^{193}Ir targets had an enrichment of 98.1%, and their thicknesses were 0.08 and 0.12 mg cm^{-2}. The momentum resolution was 0.40% and 0.06% for 25 and 202 keV electrons, respectively.

The spectrum was registered between 16 and 420 keV. The transitions at 84.28 keV, M1+18.8(6)%E2, and at 112.23 keV, M1+60.0(37)%E2, were used for electron intensity normalization with respect to the γ-intensity scale. The multipolarities were determined from the intensity ratios of the L_1-, L_2- and L_3-lines. We used the theoretical internal conversion coefficients (ICC) of Hager and Seltzer [23]. The observed conversion lines have resulted in the ICC and multipolarities reported in Table 2. The experimental conversion coefficients, as well as the theoretical values for the multipoles of interest, have been published in a separate report [19].

Conversion electrons following neutron capture were observed from 15 to 1500 keV with the spectrometer BILL [24] at ILL. The targets were 50 μg cm^{-2} thick and were enriched to 99.5% in ^{193}Ir. The neutron flux was 3×10^{14} n cm^{-2} s^{-1}. A partial evaluation of these data can be found in Table 2. In general, the data of Simonova et al. [19] (in their reevaluated form) agree satisfactorily with the results of the Grenoble measurements. There are a few exceptions where the higher resolution of the BILL spectrometer is essential, also for relatively intensive lines, an example being the 152.4 keV transition.

The multipolarity mixings obtained from the subshell data of Grenoble results for 29 intensive transitions, are listed in Table 3. The complete BILL spectrometer data in a compact form are presented in Ref. 8.

2.4. Si(Li) *detector measurements of low-energy γ-rays, and prompt and delayed γ-γ coincidences (Gatchina)*

The thermal neutron-capture γ-ray spectrum was measured at the Gatchina VVRM reactor in the energy interval 7–85 keV. A metallic target with a 93% enrichment in ^{193}Ir was exposed to an external thermal neutron beam like the one used in the coincidence measurements reported for ^{192}Ir [1]. The self-absorption intensity corrections were 50% for 23 keV, 30% for 40 keV and 10% for 60 keV. The intensity scale was calibrated with I_γ (43.1 keV) taken from Ref. 18.

All coincidence measurements with ^{194}Ir were performed with the experimental setup described in the ^{192}Ir paper, Ref. 1.

In the prompt γ-γ coincidence experiment, the target consisted of 20 mg metallic ^{193}Ir powder, enriched to 98%. The spectrometer for these measurements consisted of two HPGe-Ge(Li) planar detectors. The window of the differential discriminator

TABLE 3 (this and opposite page). Relative experimental and theoretical conver- in ^{194}Ir, measured with spectrometer BILL in Grenoble. Intensities of γ-rays (col.

E_γ (keV)	I_γ (rel.)	K	L_1	L_2	L_3	M_1
22.309						100(3) 100
27.944					100(4) 100	14.3(7) 14.71
29.890					38.9(25) 48.54	100(2) 100
34.527			100(2) 100	7.2(5) 9.90	 1.10	30.0(13) 22.78
34.829			100(2) 100	5.9(2) 6.96	58.2(16) 47.39	31.1(11)* 25.76
35.750			100(2) 100	39.7(19) 42.13	28.9(11) 37.11	23.9(9) 22.81
39.217	74.9		100(2) 100	8.5(3) 10.05	1.20(4) 1.25	24.0(13) 22.81
41.166			1.15(17) 1.43	66.4(2) 92.00	100(2) 100	 0.40
43.119	335.8		100(2) 100	10.3(3) 10.46	2.17(10)* 1.69	22.9(7) 22.79
54.404			100(2) 100	20.5(9) 11.31	7.2(4) 2.59	25.0(13)* 22.66
56.844			100(2) 100	12.1(5) 12.54	 3.83	21.7(12) 22.67
62.793	14.2		100(2) 100	9.6(3) 9.68	35.8(12)* 33.61	25.8(8)* 25.06
64.647			100(5) 100	7.8(12)* 9.77	0.82(12)* 1.04	19.4(14) 22.71
82.339	216.2		100(2) 100	11.3(5) 12.83	5.4(7) 3.81	22.8(10) 22.81
84.288	499.4		100(2) 100	68.8(31) 72.73	58.3(26) 58.14	23.0(10) 22.89
95.575	346.5	100(2)* 100	21.3(7)* 14.84	2.88(13)* 2.41	0.64(13) 0.99	5.0(2)* 3.37
109.400	26.4	64.9(29) 66.58	11.0(5) 8.07	100(2) 100	97(6)* 82.96	10.4(24) 1.96
112.23	870.5	100(2) 100	24.8(8)* 13.94	66.1(19) 45.17	52.4(17)* 36.43	8.2(4) 3.22
115.473	202.3	100(5) 100	17.7(10) 14.84	2.07(9) 1.76	 0.41	4.35(12) 3.37
117.880	185.6	100(5) 100	20.0(11) 14.83	2.5(2) 2.00	 0.60	4.0(3) 3.37

sion coefficients for $K, L_1, L_2, L_3, M_1, M_2, M_3, N_1$ and $N_{2,3}$ subshells of transitions 2) are given for lines measured with GAMS spectrometers.

E_γ (keV)	M_2	M_3	N_1	$N_{2,3}$	Multipolarity
22.309	10.3(6)*	1.5(2)	14.6(4)		M1
	10.72	1.22	30.17	3.59	
27.944	14.6(8)	17.8(10)	1.7(3)*	6.52(10)	M1+6.3(6)% E2
	22.51	25.31	4.35	14.94	
29.890	16.1(5)	10.2(6)	18.8(6)	4.5(8)	M1+0.49(5)% E2
	20.03	12.26	29.29	9.79	
34.527	3.2(3)*		3.9(3)		M1
	2.44	0.27	6.60	0.78	
34.829	2.41(13)*	15.4(4)	8.3(2)	4.7(2)	M2
	2.03	12.75	8.14	4.55	
35.750	13.4(9)	7.3(7)*	4.2(10)		M1+2.5(2)% E2
	10.39	9.43	6.59	5.95	
39.217	4.6(5)	0.20(4)	5.02(14)		M1+0.014(6)% E2
	2.48	0.31	6.55	0.79	
41.166	20.9(8)	25.8(7)		14.4(16)	E2
	22.77	25.52	0.13	14.30	
43.119	2.48(7)	0.27(2)*	5.54(16)	0.68(3)	M1+0.064(11)% E2
	2.58	0.42	6.50	0.86	
54.404	2.5(2)*	0.25(5)*	7.9(7)	1.9(3)	M1+0.26(4)% E2
	2.81	0.66	6.34	0.97	
56.844	2.9(4)		5.0(4)*		M1+0.5(2)% E2
	3.12	0.97	6.30	1.14	
62.793	2.8(3)*	11.9(3)	6.7(3)*	3.5(4)	M2
	2.63	9.00	7.27	3.30	
64.647	5.6(6)		6.7(4)		M1
	2.44	0.26	6.22	0.74	
82.339	4.8(4)		8.1(5)		M1+1.1(2)% E2
	3.21	0.98	6.21	1.15	
84.288	18.5(8)	16.3(7)	6.0(2)*	9.9(10)	M1+19.7(8)% E2
	18.16	15.05	6.24	9.17	
95.575	0.93(8)	0.75(13)	1.26(5)		M1+3.0(3)% E2
	0.60	0.25	0.92	0.24	
109.400	27.0(32)	26.2(19)		13.9(28)	E2
	25.03	21.52	0.54	12.74	
112.23	17.9(5)	14.8(4)	1.42(17)	8.23(23)	M1+72.9(21)% E2
	11.31	9.46	0.88	5.66	
115.473			1.0(4)		M1+1.4(4)% E2
	0.44	0.10	0.92	0.15	
117.880			1.43(9)		M1+2.5(7)% E2
	0.50	0.15	0.91	0.18	

Table 3. (continued)

E_γ (keV)	I_γ (rel.)	K	L_1	L_2	L_3	M_1
123.845	434.9	100(5)	18.0(10)	2.01(11)		4.08(22)
		100	14.82	1.73	0.38	3.36
132.883	75.6	100(6)	20.4(13)	54.6(35)	45.0(28)	
		100	12.85	55.53	42.46	2.97
138.686	348.4	100(6)	17.2(11)	32.4(20)	23.9(15)	5.24(35)*
		100	13.82	25.85	18.96	3.17
148.934	615.8	100(7)	13.9(12)*	82(6)*	62.5(46)	4.4(5)
		100	11.58	70.36	52.00	2.69
152.405	158.1	100(7)	25.8(26)	82(9)	58.4(43)	12.8(18)
		100	11.60	67.03	49.13	2.69
160.825	145.7	100(9)	14.4(16)	20.7(21)*	17.9(21)*	
		100	13.68	22.09	15.29	3.13
160.996	180.7	100(15)	18.8(28)	5.4(10)	2.5(5)*	4.6(8)
		100	14.61	4.47	2.37	3.34
184.687	395.7	100(6)	20.0(13)	76.5(48)	51.2(40)*	5.1(6)
		100	11.92	46.18	31.28	2.72
195.519	89.9	100(10)	10.6(26)*	61(7)	39.8(46)	
		100	12.02	41.63	27.47	2.74

* Intensity of admixture lines was subtracted.

was set successively on different transitions and nearby regions of the γ-spectrum in order to subtract the background. The results of γ-γ coincidence measurements are presented in Table 4. Energies of the "gate" lines are given and the "display" indicates the transition energies observed with the Ge(Li) detector. Precise energies, taken from the GAMS data (Table 2), are given in the third column. The initial and final states, connected by the transition observed in the coincidence spectra, are shown in the last two columns.

In order to search for isomeric γ-transitions with energies between 30 and 500 keV, an energy-time experiment was performed in the range from 5 to 3000 ns. One of the Ge(Li) detectors was replaced by an organic scintillator. Signals from that detector, corresponding to $E_\gamma \approx 1.5$ MeV, were used to start the time-to-amplitude converter, while the HPGe signals stopped it. The resolving time of the system was about 15 ns at E_γ(HPGe) = 50 keV. No new isomeric transition of interest was discovered in this experiment.

A search was made for transitions populating the $T_{1/2} = 31.85$ ms, 147.1 keV $J^\pi = 4^+$ isomeric level. The aim of this experiment was to discover positive pa- rity states connected to that level by γ-transitions, which are expected to be of M1 or E2 multipolarity in most cases. The isomeric state is depopulated (see Fig. 1) by two strongly converted M2 transitions with energies of 34.8 and 62.8 keV to the 84.3 and 112.2 keV 2^- states. The latter decay to the ground state by the M1+E2

(this and opposite page)

E_γ (keV)	M_2	M_3	N_1	$N_{2,3}$	Multipolarity
123.845	0.70(8) 0.43	 0.097	 0.91	 0.14	M1+1.4(4)% E2
132.883	13.6(10) 13.91	10.8(14)* 11.05	 0.80	4.8(7)* 6.65	M1+88.5(23)% E2
138.686	9.1(7)* 6.48	5.65(46)* 4.94	1.4(2) 0.84	3.9(4) 3.02	M1+67.8(23)% E2
148.934	22.7(16) 17.67	18.8(14) 13.54	 0.71	11.6(15) 8.20	E2
152.405	21.7(25) 16.84	17.2(28) 12.79	 0.71	7.2(14) 7.77	E2
160.825	9.7(12) 5.56	6.0(11)* 4.21	 0.82	1.77(34) 2.49	M1+71(7)% E2
160.996	2.5(6) 1.12	1.25(27)* 0.62	1.25(24) 0.88	 0.46	M1+20(4)% E2
184.687	17.6(12) 11.62	12.3(26)* 8.14	 0.71	3.9(9) 5.14	E2
195.519	9.9(21) 10.46	6.7(11)* 7.15	 0.71	5.9(13)* 4.58	E2

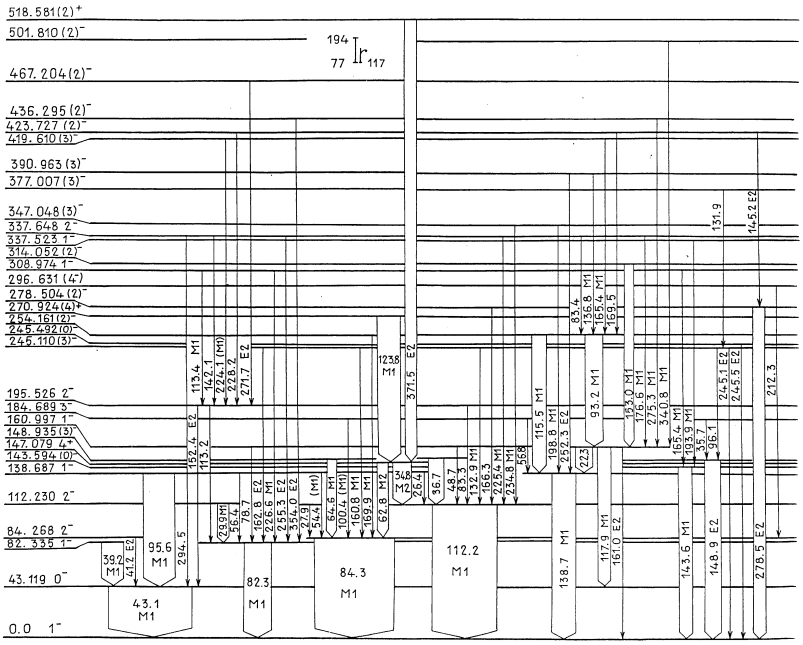

Fig. 1. Partial level scheme of ^{194}Ir.

TABLE 4. Results of the γ-γ coincidence experiments.

(A) Prompt γ-γ coincidences

Gate $E_{\gamma 1}$ (keV)	Display $E_{\gamma 2}$ (keV)	[a] E_γ (keV)	E_i (keV)	E_f (keV)
43.1	92.8(5)	93.166	254.2	161.0
	95.3(3)	95.575	138.7	43.1
	115.1(3)	115.473	254.2	138.7
	117.1(3)	117.880	161.0	43.1
	152.1(3)	152.405	195.5	43.1
	181.0(3)	-	-	-
	(226.9(3))	226.639	309.0	82.3
	(275.4(3))	275.292	436.3	161.0
	340.8(3)	340.813	501.8	161.0
	371.0(3)	-	-	-
	418.4(3)	-	-	-
84.3	161.5(3)	160.825	245.1	84.3
	282.9(3)	-	-	-
	338.2(3)	-	-	-
	342.2(3)	-	-	-
112.2	121.9(3)	-	-	-
	129.3(3)	-	-	-
	132.8(3)	132.883	245.1	112.2
	165.2(3)	165.448	419.6	254.2
	234.6(2)	234.817	347.0	112.2
	245.5(3)	-	-	-
	264.8(2)	264.744	376.97	112.2
123.8	99.9(4)	100.353	371.3[b]	270.9
	(129.5(5))	129.571	542.6[b]	413.0
	136.4(4)	136.100	407.0[b]	270.9
	153.3(5)	152.960	524.2[b]	371.3
	249.3(3)	248.599	519.5[b]	270.9
	271.7(3)	271.676	542.6[b]	270.9
148.9	138.9(2)	-	-	-
	145.4(2)	-	-	-
	(189.5(2))	-	-	-
	(204.9(3))	-	-	-
152.4	117.5(3)	117.880	161.0	43.1
153.0	139.0(3)	-	-	-
	(184.7(3))	-	-	-
	216.5(3)	-	-	-
	218.9(3)	-	-	-
	241.4(3)	-	-	-
184.7	460.3(3)	-	-	-
278.5	145.2(3)	145.221	423.7	278.5

Table 4. (continued)

(B) Delayed γ-γ coincidences[c]

Gate $E_{\gamma 1}$ (keV)	Display $E_{\gamma 2}$ (keV)	[a] E_γ (keV)	E_i (keV)	E_f (keV)
Ir K X-rays	100.4	100.353	371.3[b]	270.9
	123.8	123.845	270.9	147.1
	129.6	129.571	542.6[b]	413.0
	142.1	142.119	413.0[b]	270.9
	271.5	271.676	542.6[b]	270.9
	371.5	371.502	518.6	147.1

[a] See Table 2.

[b] These levels are included in the level scheme mainly on the basis of coincidence data.

[c] This experiment was made in order to search for the population of the 32 ms isomeric state. The display shows the energies of lines (in keV) detected in the HPGe detector.

transitions whose K-conversion coefficients are 10.3 and 3.8, respectively. The Ir Kα X-rays, which accompany the decay of these 2^- states, were used in this experiment to select isomeric decay processes. The measurements were performed with the HPGe detector and a NaI(Tl) scintillator. The window of a differential discriminator was set on the part of the NaI(Tl) γ-ray spectrum, corresponding to the K X-ray line. A part of this line is related to K-conversion of the 84.3 and 112.2 keV transitions and is delayed with respect to the γ-rays registered in the HPGe detector.

The γ-spectrum, gated by K X-ray events electronically delayed by 5 to 75 ms with respect to pulses from the HPGe detector, was stored in the multichannel analyzer. In order to minimize the chance-coincidence events, the two detectors were placed as close as possible to a metallic ^{193}Ir target of a few milligrams, and the neutron beam was diaphragmed by ^{6}LiF. The counting rates in the detectors did not exceed 200 counts/s. Chance coincidences were taken into account.

The γ-transitions listed in the second part of Table 4 are observed to populate the 32 ms isomeric state. The display of both parts of Table 4 is similar. From these results it is possible to construct system of positive parity levels not observed in the (d,p) reaction and/or via the primary neutron capture spectrum.

2.5. The reaction ^{193}Ir(d,p)^{194}Ir (Munich)

The ^{193}Ir(d,p) reaction spectrum was measured at the Tandem Accelerator of the University and Technical University of Munich in Garching. The target consisted of ^{193}Ir enriched to 98%. It had an area of $1 \times 4\text{mm}^2$ and its thickness was 35 μg cm^{-2} on a 5 μg cm^{-2} thick carbon backing. A deuteron beam of energy $E_d = 22$ MeV was used.

Protons were detected in a gas-filled light-ion detector [25] in the focal plane of the high resolution Q3D spectrograph [26]. After the entrance foil, an incident particle passes a multiwire proportional chamber, consisting of two anode wires between a cathode plane foil and a cathode strip foil. The energy-loss signal is obtained from the anode wires. The particle is stopped in a plastic scintillator which yields the rest-energy signal. The

type of the incident particle can be identified by combining the energy loss with the rest-energy signal. Energy of the particle is determined by its position in the focal plane of the spectrograph. Uncertainty of the intrinsic position is less than 0.1 mm. Depending on the magnetic field of the spectrograph, relative energies can be determined to a precision as good as 0.1 keV.

For protons, angular distributions at four angles from $20°$ to $50°$ were measured. The elastic-scattering line was observed by a solid-state monitor detector. Intensities of the lines in the position sensitive detector were normalized using data from the monitor counter. Weighted mean values for level energies and their errors were computed from the data at all four angles. The results are listed in Table 5.

3. Discussion

A level scheme, based on the above described results as well as on the complementary experimental results, is presented in Ref. 8. The attempt has been made to interprete this level scheme in terms of the rotor-plus-two-quasiparticles model, for all levels up to the 340 keV excitation energy and for a few higher-lying levels.

Here, we present only a partial level scheme (see Fig. 1). This level scheme illustrates mainly the use of the results of Table 2. The multipolarities and spins shown in Fig. 1 are based on the Riga-Salaspils conversion electron spectra. In a few cases (e.g., the 152.4 keV line), multipolarities were updated with regard to the Grenoble results.

From the data on neighbouring nuclei ^{191}Ir, ^{193}Ir, ^{193}Os, a number of low-lying negative-parity bands with $K = 0, 1, 2$ and 3, and also a few positive parity bands are predicted in ^{194}Ir. They are built on the Nilsson proton orbits $3/2^+[402]$, $1/2^+[400]$ and $11/2^-[505]$, and neutron orbits $3/2^-[512]$, $1/2^-[510]$ and $11/2^+[615]$. The detailed analysis of all obtained results (see Ref. 8) allowed the identification of 9 negative parity bands, or band heads, and 3 positive parity band heads, including the 518 keV 2^+ band head, probably representing a γ-vibration on the 147.0 keV 4^+ level.

Odd-odd nuclei can be described within the framework of the interacting boson-fermion-fermion model (IBFFM) [27–31], which couples the valence-shell proton and neutron quasiparticles to the even-even core described in the interacting boson model (IBM) [32]. The corresponding computer code IBFFM [33] allows the calculation of energy spectra, electromagnetic properties, spectroscopic strengths in transfer reactions and spectral distributions. Recently, such calculations were performed for the low-lying (up to 0.5 MeV) negative parity levels in ^{194}Ir and for their (d,p) spectroscopic strengths [12]. The boson core was fitted to the low-lying levels of the even-even nucleus ^{196}Pt using the O(6) limit of IBM which is applicable in the Os-Pt region [34–36]. Then, in analogy to the previous calculation for ^{192}Ir [1], the O(6) parameters were renormalized to the total boson number $N = 4$. The full account of these calculations one can find in Ref. 8.

TABLE 5. Level excitation energies and relative differential cross-sections (in relative units) observed in the ^{193}Ir(d,p)^{194}Ir *reaction.*

E_{exc}	dE_{exc}	$d\sigma/d\Omega$, $E_d = 22$ MeV			
(keV)	(keV)	20°	30°	40°	50°
0.10	0.16	168(13)	133(13)	98(13)	55(5)
43.06	0.16	138(11)	118(14)	89(12)	50(5)
83.88	0.08	975(70)	850(70)	560(60)	343(24)
112.22	0.08	955(60)	685(60)	555(60)	333(23)
138.4	0.3	203(20)	137(18)	62(12)	5
148.75	0.13	610(40)	430(40)	340(40)	193(17)
161.14	0.13	490(40)	448(40)	314(37)	179(17)
192.70	0.10	20	18(5)	10	10(3)
244.4	0.4	89(15)	63(9)	47(10)	30(5)
255.1	0.3	106(16)	77(11)	54(11)	37(6)
278.74	0.12	475(40)	303(28)	345(40)	208(16)
296.34	0.10	1030(70)	570(50)	565(60)	287(21)
311.6	0.4	103(16)	70(10)	58(11)	37(7)
337.4	0.4	195(30)	118(19)	114(19)	62(11)
346.76	0.19	455(50)	370(40)	240(31)	156(16)
376.76	0.11	1010(70)	740(60)	645(70)	359(26)
393.0	0.12	20	18(8)	16(7)	11(5)
422.15	0.16	306(23)	204(19)	145(24)	87(8)
433.9	0.4	66(9)	31(7)	33(6)	27(21)
467.7	0.4	33(5)	28(5)	23(7)	17(4)
489.55	0.18	195(12)	114(9)	90(11)	64(6)
501.9	0.3	75(8)	41(6)	34(6)	22(7)
522.5	0.4	68(7)	17(3)	10(3)	9(2)
545.37	0.16	217(13)	119(9)	105(11)	62(5)
557.8	0.5	39(7)	19(4)	20(5)	11(4)
572.4	0.7	15	23(7)	33(10)	5
578.97	0.23	94(15)	94(8)	61(14)	46(8)
591.9	0.4	15	39(5)	27(5)	12(3)
605.73	0.17	48(10)	64(6)	44(7)	25(3)
619.9	0.4	14(5)	63(6)	38(5)	22(4)
639.55	0.21	38(5)	74(7)	54(6)	28(10)
656.42	0.22	78(10)	77(8)	49(6)	29(4)
667.5	0.4	51(7)	66(7)	46(6)	23(7)
677.49	0.23	80(8)	94(9)	56(7)	49(4)
694.5	0.5	11(4)	31(4)	29(6)	11(2)
707.7	0.4	36(5)	40(5)	29(7)	17(6)
719.1	0.4	31(4)	26(4)	25(6)	18(2)
746.3	0.3	X	50(6)	58(12)	40(5)
759.0	0.3	X	56(7)	80(15)	54(6)
772.6	0.4	X	41(6)	23(6)	32(4)

Table 5. (continued)

E_{exc}	dE_{exc}	$d\sigma/d\Omega$, $E_d = 22$ MeV			
(keV)	(keV)	20°	30°	40°	50°
799.7	0.8	X	11(3)	35(12)	10
808.7	0.3	188(19)	88(10)	70(15)	83(15)
819.2	0.3	X	68(9)	74(14)	85(16)
834.2	0.9	X	15(4)	11(4)	10
853.8	0.4	X	27(5)	28(8)	41(9)
872.4	0.3	X	63(13)	72(14)	36(10)
879.4	0.6	X	45(12)	38(11)	52(12)
888.00	0.14	X	10(4)	10	13(4)
897.4	0.5	X	34(5)	28(8)	21(6)
908.2	0.6	10	17(4)	18(6)	17(4)
921.2	0.5	10	17(3)	10	19(4)
934.0	0.8	10	20(6)	12(4)	7(3)
948.11	0.18	283(21)	283(23)	141(20)	149(14)
965.9	0.7	10	31(7)	22(6)	12(4)
1001.2	0.4	31(6)	55(8)	30(7)	30(6)
1029.6	0.23	171(14)	130(14)	90(14)	85(10)
1044.5	0.8	10	27(7)	21(7)	12(5)
1062.5	0.4	55(7)	42(6)	44(9)	27(6)
1074.0	0.3	145(13)	114(12)	88(14)	75(9)
1087.5	0.3	88(11)	54(9)	65(11)	39(7)
1095.6	0.7	54(9)	25(7)	10	10
1105.8	0.4	44(9)	41(5)	43(9)	34(6)
1115.2	0.6	72(11)	40(6)	10	10
1122.1	0.4	46(9)	35(5)	45(9)	25(6)
1134.5	0.4	83(8)	55(6)	43(9)	21(5)
1146.7	0.3	88(8)	58(6)	42(9)	35(6)
1161.7	0.3	85(8)	24(6)	48(9)	45(7)
1179.6	0.3	53(6)	37(4)	30(6)	34(6)
1198.10	0.24	223(20)	117(11)	107(15)	95(11)
1211.1	0.6	79(13)	51(7)	-	32(8)
1222.7	0.4	111(6)	81(9)	-	79(11)
1234.6	0.6	60(14)	37(6)	-	24(6)
1249.8	0.5	58(16)	41(6)	-	57(8)
1258.0	0.9	34(15)	59(7)	-	-

4. Conclusions

The results presented here on the measurements of the ^{193}Ir(n$_{th}$, γ)^{194}Ir and ^{193}Ir(d,p)^{194}Ir reactions represent a part of data obtained in a larger collaboration. They include details important for the construction of the level scheme and for the assignment of the spins and parities. Since the main paper [8] is already very long, this information is published separately. The factors supporting publication of these data are: (i) isotopic

identification of the lines detected in the Fribourg-Wuerelingen and Riga-Salaspils measurements shows with high certainty that they are due to ^{194}Ir, and not ^{195}Ir from double neutron capture; (ii) the earlier (n_{th}, γ_{low}) measurements, although less sensitive, present somewhat more reliable γ-intensity scale for intensive low-energy transitions between 43 and 112 keV.

The good agreement observed between the data taken in Wuerenlingen and Grenoble indicates that there are no systematic errors and that the quoted uncertainties are realistic. This is not quite obvious for such complicated spectra. We note a few discrepancies which can be explained by the differences in energy resolution.

Acknowledgements

We thank our colleagues from the Kiev group (A. V. Murzin and V. A. Libman) for the fruitful collaboration. All their data have been included in the forthcoming ^{194}Ir paper [8].

The authors of the Rīga group are grateful to the German Volkswagen Stiftung and the Soros Foundation Latvia for their financial support. This work was also supported by the Swiss National Science Foundation.

References

1) J. Kern et al., Nucl. Phys. A **534** (1991) 77;

2) H. Krueger, H. Hanle, M. Koriath and K. Stelzer, Nucl. Phys. A **169** (1971) 363;

3) R. G. Helmer, Phys. Rev. **137** (1965) B232;

4) N. R. Johnson and W. N. Bishop, Nucl. Phys. **69** (1965) 131;

5) D. C. Williams and P. A. Naumann, Phys. Rev. **135** (1964) B289;

6) A. Lundan and A. Siivola, Nucl. Phys. A **106** (1968) 417;

7) C. Heiser, H. F. Brinckmann and W. Fromm, Nucl. Phys. A **115** (1968) 213;

8) M. Balodis et al. (to be published);

9) M. K. Balodis, In: *Proc. 6th Int. Symp. Neutron Capt. Gamma Ray Spectr.*, Leuven 1987 (Inst. Phys. Conf. Ser. 88, 1988) S526;

10) M. K. Balodis, T. V. Guseva, and J. Kern, Izv. Akad. Nauk SSSR, ser.fiz. **52** (1988) 37;

11) M. Balodis and the ^{194}Ir collaboration, In: *Proc. 8th Int. Symp. Neutron Capt. Gamma Ray Spectr.*, Fribourg 1993 (World Scientific, Singapore, 1994) 355;

12) P. E. Garrett, D. G. Burke, Tao Qu, V. Paar and S. Brant, Nucl. Phys. A **579** (1994) 103;

13) B. Michaud, J. Kern, L. Ribordy and L. A. Schaller, Helv. Phys. Acta **45** (1972) 93;

14) O. Piller, W. Beer and J. Kern, Nucl. Instr. Meth. **107** (1973) 61;

15) W. Beer, J. Kern and O. Piller, Nucl. Instr. Meth. **107** (1973) 79;

16) W. Schwitz and J. Kern, In: *Proc 2nd Int. Symp. Neutron Capt. Gamma Ray Spectr.*, Petten 1974, p.697;

17) A. Raemy, W. Beer, J.-Cl. Dousse, R. Eichler, J. Kern, Th. von Ledebur and W. Schwitz, Helv. Phys. Acta **49** (1976) 645;

18) A. Raemy, J.-Cl. Dousse, J. Kern and W. Schwitz, *Report of the Physics Department*, University of Fribourg, Switzerland, IFP-SP-006 (1975) (unpublished);

19) L. I. Simonova, N. D. Kramer and P. T. Prokofjev, Report of the Physics Institute, Riga-Salaspils, LAFI-010 (1979);

20) G. G. Colvin, J. A. Cizewski, H. G. Borner, P. Geltenbort, F. Hoyler, S. A. Kerr and K. Schreckenbach, *Report ILL Grenoble* N 86Co09T (1986);

21) B. Singh, Nucl. Data Sheets **56** (1989) 75;

22) M. K. Balodis, V. A. Bondarenko and P. T. Prokofjev, Izv. Akad. Nauk SSSR, ser.fiz. **28** (1964) 262;

23) R. C. Hager and E. C. Seltzer, Nucl. Data Tables **4A** (1968) 155;

24) W. Mampe, K. Schreckenbach, D. Jeuch, B. P. K. Maier, F. Braumandl, J. Larysz and T. von Egidy, Nucl. Instr. Meth. **175** (1978) 401;

25) H. Lindner, H. Angerer and G. Hlawatsch, Nucl. Instr. Meth. A **273** (1984) 444;

26) M. Loffler et al., Nucl. Instr. Meth. **111** (1973) 1;

27) S. Brant, V. Paar and D. Vretenar, Z. Phys. A **319** (1984) 355;

28) V. Paar, D. K. Sunko and D. Vretenar, Z. Phys. A **327** (1987) 291;

29) V. Paar, in *Capture Gamma-Ray Spectroscopy and Related Topics*, AIP Conf. Proc. 125 (American Institute of Physics, New York, 1985) 70;

30) V. Paar, in *In-Beam Nuclear Spectroscopy* (Akademia Kiado, Budapest, 1984) 675;

31) U. Mayerhofer et al., Nucl. Phys. A **492** (1989) 1;

32) A. Arima and F. Iachello, Phys. Rev. Lett. **35** (1975) 157; A. Arima and F. Iachello, Ann. Phys. **123** (1979) 468;

33) D. Vretenar, S. Brant and V. Paar, Computer code IBFFM/OTQM, IKP Jülich (1985);

34) J. A. Cizewski, R. F. Casten, G. J. Smith, M. L. Stelts, W. R. Kane, H. G. Boerner and W. F. Davidson, Phys. Rev. Lett. **40** (1978) 167;

35) R. J. Bijker, A. E. L. Dieperink, O. Scholten and R. Spannhoff, Nucl. Phys. A **344** (1980) 20;

36) M. Vergnes, G. Rotbard, J. Kalifa, G. Berrier-Rons, J. Vernotte, R. Setz and D. G. Burke, Phys. Rev. Lett. **46** (1981) 584.

PROUČAVANJE ^{194}Ir UHVATOM TERMIČKIH NEUTRONA I (d, p) REAKCIJOM

Proučavala su se stanja u ^{194}Ir reakcijama ^{193}Ir(n, γ) i ^{193}Ir(d, p). Mjerenja uhvata termičkih neutrona načinjena su uz reaktore u Grenoblu, Wuerenlingenu i Salapsisu. Za mjerenja γ-zračenja visoke energije upotrebljavao se spektrometar parova, a za niske energije difraktometar. Konverzijske elektrone se mjerilo magnetskim spektrometrom. Mjerenja reakcije (d, p) visokog razlučivanja izvedena su magnetskim spektrometrom. Usporedbe tih mjerenja omogućile su pouzdano izotopno prepoznavanje prijelaza u ^{194}Ir, a spektri konverzijskih elektrona i odredivanje multipolnosti prijelaza. Dobiveni su podaci osnova sheme raspada ^{194}Ir.